LANGMUIR

pubs.acs.org/Langmuir Article

Designed Amyloid Fibers with Emergent Melanosomal Functions

Hyeyeon Park,[‖] Hyeri Jeon,[‖] Min Young Lee, Hyojae Jeon, Sunbum Kwon,* Seungwoo Hong,* and Kyungtae Kang*

Cite This: *Langmuir* 2022, 38, 7077−7084 Read Online

ACCESS | Metrics & More | Article Recommendations | Supporting Information

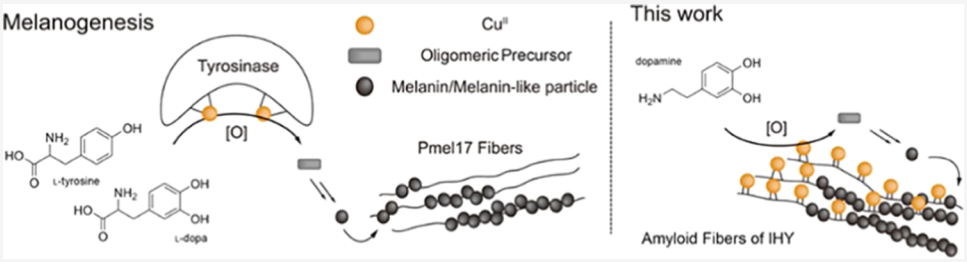

ABSTRACT: Short peptides designed to self-associate into amyloid fibers with metal ion-binding ability have been used to catalyze various types of chemical reactions. This manuscript demonstrates that one of these short-peptide fibers coordinated with Cu^{II} can exhibit melanosomal functions. The coordinated Cu^{II} and the amyloid structure itself are differentially functional in accelerating oxidative self-association of dopamine into melanin-like species and in regulating their material properties (e.g., water dispersion, morphology, and the density of unpaired electrons). The results have implications for the role of functional amyloids in melanin biosynthesis and for designing peptide-based supramolecular structures with various emergent functions.

INTRODUCTION

Self-assembly is frequently found in the natural fabrication of materials. Complex and dynamic hierarchical structures enabled by self-assembly often exhibit superior material properties.[1−4] In many cases, the process of self-assembly entails the emergence of chemical functions that are absent in the monomeric molecular units (i.e., "emergent functions"). Generally, this is possible since supramolecular association provides an efficient way to control periodic molecular configuration at surface, which is often central to the catalytic properties of various interfaces. Inspired by natural self-assembly, numerous artificial self-assembled matters have been developed,[5−8] but those designed to have emergent functions that appear only when assembled are still rare.

Functional amyloids are a kind of sophisticated self-assembled supramolecular structures that are receiving an increasing multidisciplinary interest.[9,10] Although amyloid structures have primarily been recognized as detrimental and pathological for several decades, it is now well accepted that they are rather a form of functional molecular scaffolds prevalent in nature. The supramolecular structure of amyloids ensures useful features, including superior materials properties (e.g., physicochemical stability and high rigidity/elasticity)[11] and/or chemical functions (e.g., catalytic scaffolding, gene regulation, storing hormones, and molecular recognition).[12−14] The formation of amyloid is known to have mechanistic plasticity,[15,16] which endows it with the versatility to have a broad range of physicochemical properties depending on the context. Attempts to design artificial amyloid fibers[17−20] with emergent chemical functions, such as capturing small molecules,[21] displaying functional epitopes,[22] and enhancing mechanical strength,[23] have been made. Remarkably, when histidine was presented externally, the assembled amyloid fibers showed the ability to bind to metal cations with a conserved coordination geometry, forming a group of metal−organic complexes on their surface.[24−27] These pioneering works well demonstrate the opportunity of amyloid-based materials as a new class of emergent functional materials and at the same time a potential relevance of short-peptide aggregates in prebiotic forms of enzymes and functions. However, the number of reported emergent functions and their applications to various purposes is limited.

An example of functional amyloids having central chemical roles in biological contexts is the biosynthesis of melanin, a biological pigment composed of heterogeneous oligomeric species that stem from oxidized forms of L-dopa.[28] Here, a type of functional amyloid, the one mainly composed of a melanosomal protein (Pmel17), is synthesized by melanosomes. Since its discovery, an amyloid matrix of Pmel17 has been considered to act as a physical scaffold that sequesters

Received: April 7, 2022
Revised: May 10, 2022
Published: May 24, 2022

https://doi.org/10.1021/acs.langmuir.2c00904
Langmuir 2022, 38, 7077−7084

Scheme 1. Schematic Illustrations of (Top) In Vivo Melanogenesis in Melanosome and (Bottom) the Formation of Melanin-Like Species with Cu^{II}-Coordinated Amyloid Fibers[a]

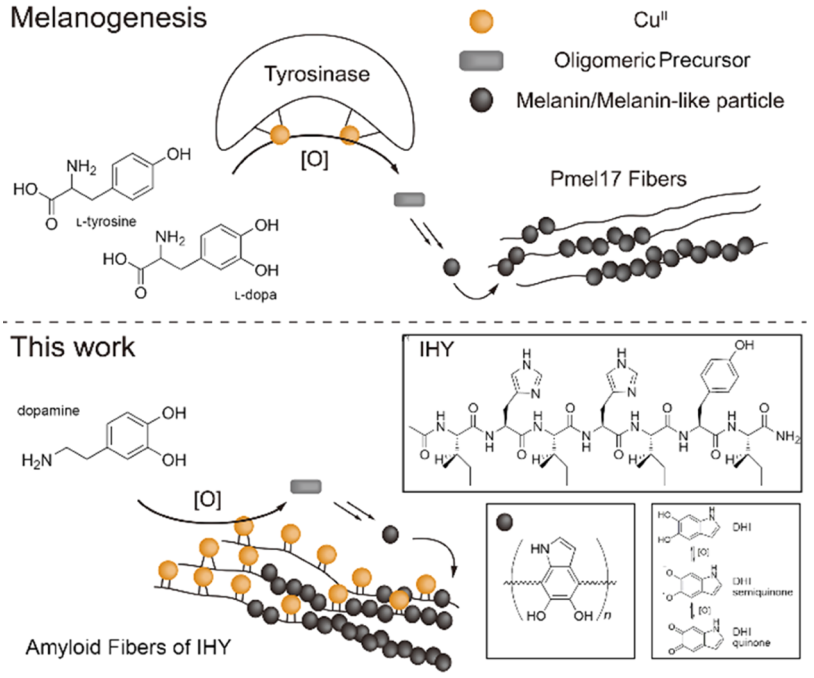

[a]The amyloid fibers in both cases can work simultaneously as an oxidation catalyst and a supramolecular template for the association.

potentially harmful molecular intermediates of melanin synthesis and also provides mechanical support.[29−31] In our recent work, however, we showed that Pmel17 fibers are catalytically active in the formation of melanin-like species.[32] They also altered the physical properties of the synthesized pigment: the presence of amyloid fibers led to more compact and water-dispersible melanin-like species in comparison to those synthesized without. These results have prompted us to design a simpler version of an amyloid-based functional scaffold that can recapitulate melanosomal functions.

RESULTS AND DISCUSSION

We envisioned that functional amyloid rationally designed to present densely populated Cu^{II} binding sites on its surface would have multiple emergent properties akin to melanosomal functions. Like Pmel17 matrix, Cu^{II} is indispensable in melanogenesis, since its redox activity is exploited by an enzyme (tyrosinase), which is responsible for the ortho-hydroxylation of tyrosine (i.e., the formation of L-dopa) and its further oxidation.[33] We, thus, expected that Cu^{II}-bound amyloid fibers would simultaneously recapitulate functional features of Pmel17 matrix and tyrosinase, making them an optimized scaffold for facilitating the formation of melanin-like species.

We used a short peptide previously designed to self-assemble into an amyloid structure with metal-coordinating ability[25] and examined the influences of Cu^{II}-coordinated amyloid fibers in facilitating catechol oxidation and their subsequent oxidative association (Scheme 1). Our results show that Cu^{II} is in synergy with the amyloid structure itself for accelerating the formation of melanin-like species. They also suggest that the peptide fibers have emergent properties to regulate various materials properties of melanin-like species composited with them.

As a model peptide, we adopted a short amyloid-forming sequence (AcNH-IHIHIYI-$CONH_2$; IHY). This peptide (and its derivatives) has been reported to bind to various metal cations after or during fibrillization, which together exhibited catalytic activities for different types of chemical reactions.[24−26] IHY was synthesized through the conventional manual solid-phase peptide synthesis (Figure S1). Aggregation of IHY into amyloid fibers was confirmed by transmission electron microscopy (TEM) and circular dichroism (CD) and Fourier transform infrared (FTIR) spectroscopy. CD spectra of IHY with or without Cu^{II} show the signature of the β-sheet structure (i.e., negative ellipticity around 220 nm, Figure 1a), indicating that amyloid fibers are formed instantaneously regardless of Cu^{II}. The presence of Cu^{II} leads to an increase in band intensity, indicating the formation of more matured cross β-sheet structures. This implies the supportive role of Cu^{II} in the formation of amyloid fibers. The amide I bands (around 1625 cm^{-1}) in the IR spectra of IHY fibers also confirm the formation of amyloid fibers through interstrand hydrogen bonds regardless of the presence of Cu^{II} (Figure S2). Likewise, TEM images of Cu^{II}-bound IHY fibers (Cu^{II}-IHY) show a characteristic morphology of amyloid fibers with a width of 10−12 nm (Figure 1a, inset).

Previously, Cu^{II}-IHY was shown to catalyze the oxidation of 2,6-dimethoxyphenol and the hydrolysis of paraoxon,[25,26] which motivated us to expect that Cu^{II}-IHY fibers would also be functional for the oxidation of catechol-containing molecules and their subsequent melanin-like association. First, we used 3,5-di-*tert*-butylcatechol (3,5-DBcat) as a probe for catechol oxidation. An oxidized form of 3,5-DBcat (3,5-di-*tert*-benzoquinone) exhibits a distinctive absorbance band at the visible range, and the oxidation is not spontaneous without a catalyst (Figures 1b and S3). The oxidation of 3,5-DBcat is significantly accelerated with the presence of Cu^{II}-IHY (Figure 2a). Cu^{II} and IHY fibers (Figure S3) are independently active

https://doi.org/10.1021/acs.langmuir.2c00904
Langmuir 2022, 38, 7077−7084

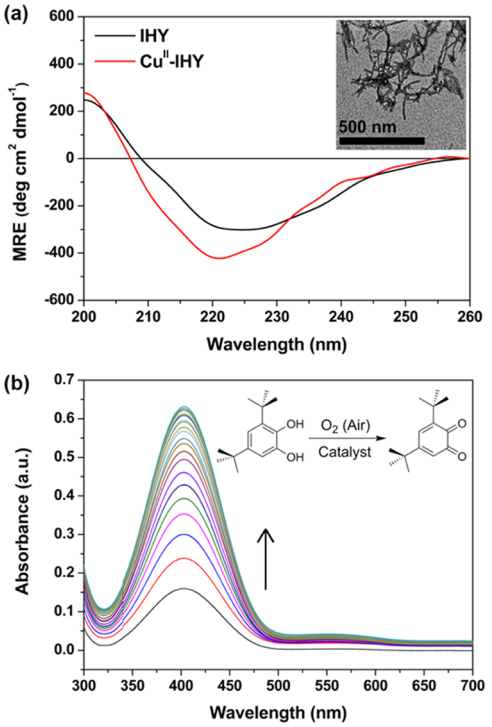

Figure 1. (a) CD spectra of Cu^{II}-IHY and IHY. (inset) TEM image of Cu^{II}-IHY aggregated into amyloid fibers. The data indicate the formation of amyloid fibers regardless of the presence of Cu^{II}. (b) Gradual increase in absorbance at 405 nm of 3,5-DBcat (400 μM) in the presence of 20 μM Cu^{II}-IHY. The spectra have been collected every 10 min. The inset shows the oxidation of 3,5-DBcat.

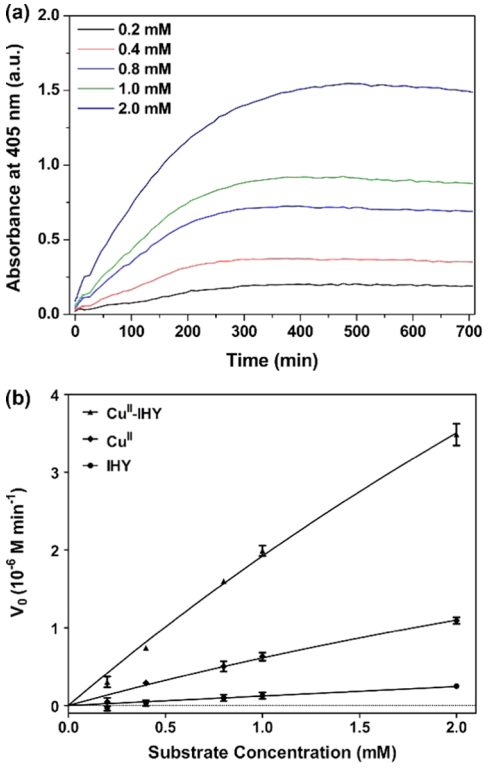

(c)

Catalyst	k_{cat}/K_m (M^{-1} min^{-1})	k_{cat} (min^{-1})	K_m (mM)	V_{max} (M min^{-1})
Cu^{II}-IHY	106.68±6.93	1.26±0.81	12.11±8.03	5.548×10^{-5}
Cu^{II}	34.52±2.87	0.28±0.06	8.18±2.05	2.016×10^{-5}
IHY	15.25±8.37	0.02±0.004	1.428±0.55	4.355×10^{-7}

Figure 2. (a) Time-dependent change of absorbance at 405 nm of samples containing various concentrations of 3,5-DBcat with a fixed concentration of Cu^{II}-IHY (20 μM). (b) Changes in the initial rate of catalytic oxidation upon varying the substrate. The spectra were fitted to the Michaelis–Menten equation. (c) Measured kinetic parameters of 3,5-DBcat oxidation. The data show the synergistic relationship between catalytic activities of Cu^{II} and IHY.

in accelerating the reaction compared to the control reaction. Plotting the initial rate of the reaction against the concentration of the substrate at each condition clearly shows such a trend (Figure 2b), which we could fit the Michaelis–Menten model. The values of k_{cat}, K_m, and k_{cat}/K_m derived from the plot are shown in Figure 2c. For both V_{max} and k_{cat}/K_m, the values of Cu^{II}-IHY (5.548×10^{-5} M·min^{-1} and 106.68 M^{-1} min^{-1}, respectively) are higher than the sum of those of Cu^{II} and IHY (2.016×10^{-5} M·min^{-1} and 34.52 M^{-1} min^{-1} for Cu^{II}; 4.355×10^{-7} M·min^{-1} and 15.25 M^{-1} min^{-1} for IHY, respectively). The fitted data overall suggest that Cu^{II} alone is catalytically active in the oxidation of 3,5-DBcat, and the catalytic efficiency is synergistically improved when it is coordinated with IHY fibers. We note, however, that the kinetic parameters of Cu^{II}-IHY are still largely lower than those of moderate natural enzymes, as frequently seen in artificially designed enzymes.

Encouraged by the 3,5-DBcat oxidation results, we next asked if Cu^{II}-IHY could facilitate the oxidative association of catechol derivatives, reminiscent of the role of Pmel17 in melanogenesis. Dopamine, which self-associates into melanin-like species under aerobic conditions, was chosen as the simplest catecholamine. In basic, amine-based buffer solutions, dopamine spontaneously forms a thin organic film (called polydopamine) at liquid–solid interfaces, which is being explosively applied to a broad range of material fields. While adjusting to neutral pH for minimizing the spontaneous association, we added Cu^{II}, IHY fibers, and Cu^{II}-IHY to solutions of dopamine. The formation of melanin-like species (i.e., the oxidative association of dopamine) is readily recognizable by the eyes as it absorbs light broadly in the ultraviolet (UV) and visible ranges. Regardless of the presence of Cu^{II}, melanin-like species formed with IHY fibers and Cu^{II}-IHY disperse more easily than those without IHY fibers (Figure 3a). To quantitatively analyze the formation of melanin-like species, we plotted time-dependent change of absorbance at 450 nm (A_{450}) for each condition (Figures 3b and S4). The value of A_{450} has frequently been used as a quantitative measure for melanin-like species, as they exhibit characteristic monotonic and featureless light absorption in a broad range. Similar to the 3,5-DBcat oxidation results, the plot clearly shows that all of the conditions of Cu^{II}, IHY fibers, and Cu^{II}-IHY accelerate the reaction to different extents. Remarkably, the IHY fiber itself also exhibits catalytic activity. This is in line with our previous result, where amyloid fibers made of various proteins (but not their monomeric forms) exhibited catalytic properties for the association of dopamine.[32] The result with IHY fibers thus suggests that the supramolecular structure of amyloid is, at least partially, responsible for its catalytic property. As in the case of 3,5-DBcat oxidation, Cu^{II}-IHY is the best in accelerating the formation of melanin-like species, indicating that Cu^{II} and IHY fibers, when combined, are in synergy for doing so. Cu^{II} alone is almost

https://doi.org/10.1021/acs.langmuir.2c00904
Langmuir 2022, 38, 7077–7084

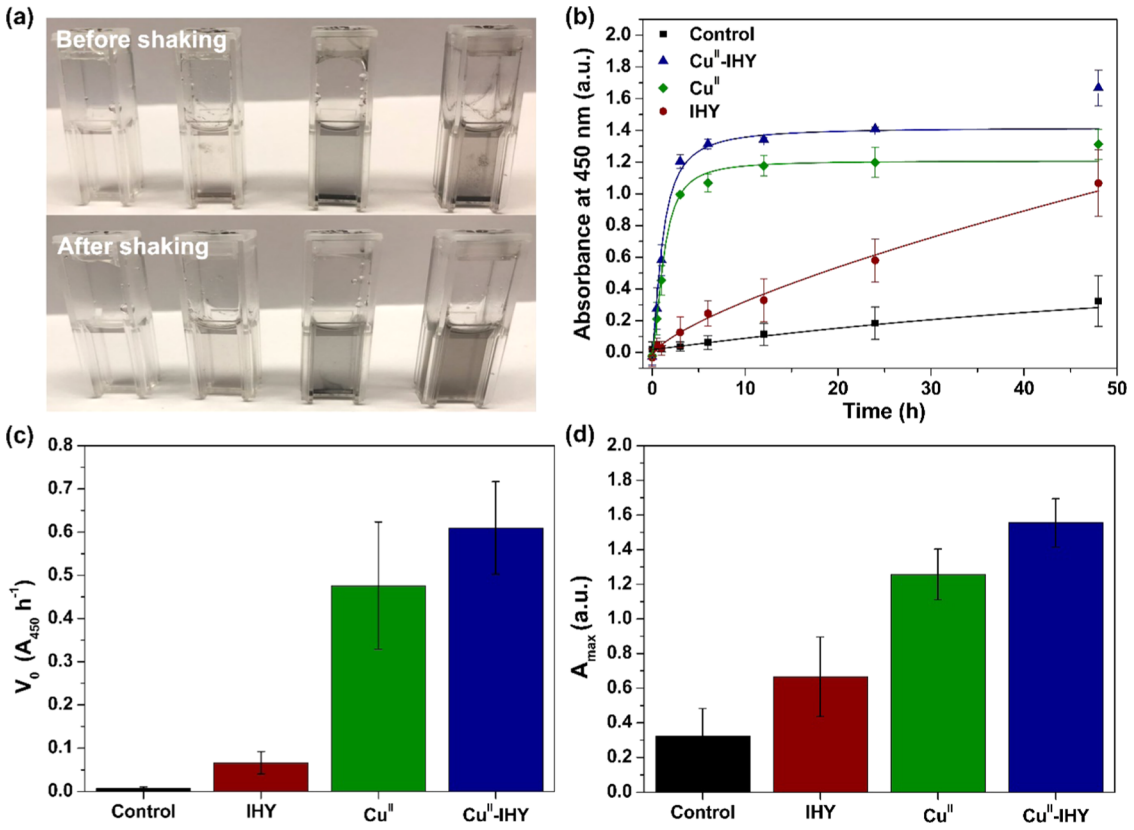

Figure 3. (a) Photograph of melanin-like species synthesized from dopamine (300 μM, pH 7.4) with no catalyst (control), IHY (300 μM), Cu^{II} (300 μM), and Cu^{II}-IHY (300 μM) (from the left). The photographs were taken before (top) and after (bottom) shaking. (b) Time-dependent changes of A_{450} values at each condition. (c,d) Values of V_0 and A_{max} measured at each condition. The data collectively show that Cu^{II}-IHY facilitates the formation of melanin-like species most effectively.

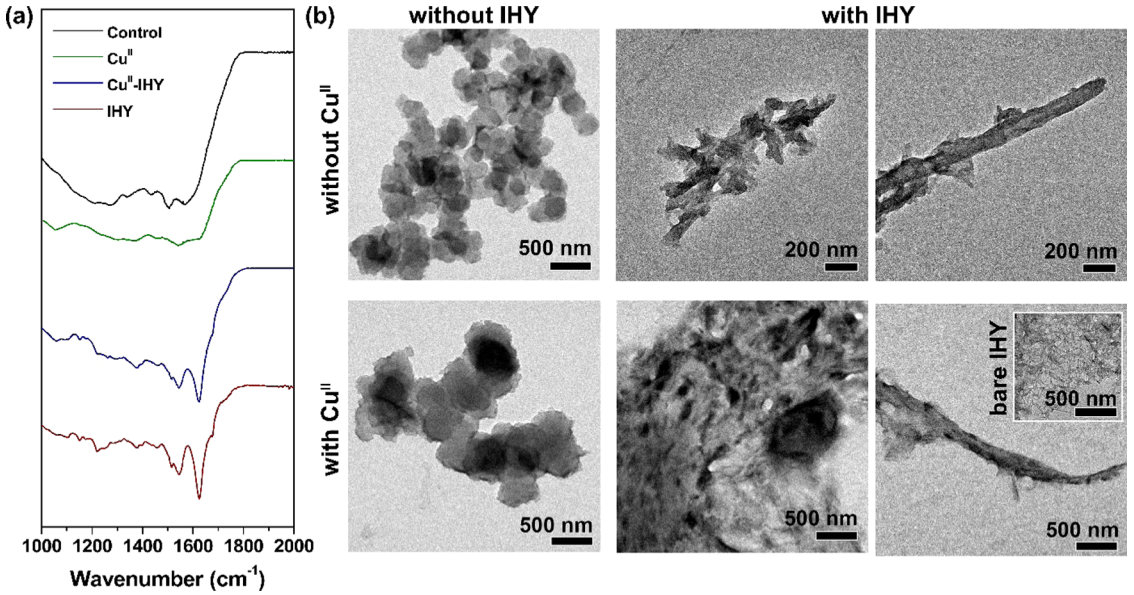

Figure 4. (a) FTIR spectra of melanin-like species synthesized from dopamine (300 μM, pH 7.4) with no catalyst (control), IHY (300 μM), Cu^{II} (300 μM), and Cu^{II}-IHY (300 μM). (b) TEM images of melanin-like species formed at each condition. The inset shows the TEM image of Cu^{II}-IHY fibers. The images suggest that IHY fibers regulate the morphology of melanin-like species.

as effective as Cu^{II}-IHY in promoting the kinetic parameters, indicating that the initial oxidation of dopamine presumably plays the most determining role in its self-association. We tried to fit temporal changes of A_{450} values at each condition to a logistic function (see the Experimental Section), according to our previous work.[32] To compare the kinetic features of the process of the oxidative association at each condition, we extracted the values of V_0, A_{max} from fitted kinetic profiles, defined as an initial increasing rate of A_{450}, and the maximum value of A_{450}, respectively. V_0 and A_{max} reflect the efficiency of

https://doi.org/10.1021/acs.langmuir.2c00904
Langmuir 2022, 38, 7077−7084

the catalyst for the initial oxidation of dopamine and its capability as a functional scaffold that can accommodate and regulate structures of melanin-like species, respectively. The values of V_0 and A_{max} increase in all of the cases with IHY fibers, Cu^{II}, or Cu^{II}-IHY, with Cu^{II}-IHY exhibiting the highest improvement (Figure 3c,d). Such trends stay unaltered when decreasing the concentrations of each catalyst (Figure S5).

In melanogenesis, the amyloid matrix in melanosomes is thought to regulate the material properties of final melanin products. We asked if the Cu^{II}-IHY complex had other functions than simply accelerating the reaction. First, we conducted FTIR spectroscopy for characterizing melanin-like species synthesized in the presence of Cu^{II}, IHY, and Cu^{II}-IHY. FTIR spectra collected from melanin-like species itself and those with Cu^{II} are primarily similar (Figure 4a), displaying bands around 1540 and 1630 cm^{-1}, consistent with previous reports.[34−36] In contrast, those collected with IHY and Cu^{II}-IHY differ critically from the others, as they contain the distinctive band of the β-sheet structure at 1625 cm^{-1}. This suggests that amyloid fibers remain structurally intact during the formation of melanin-like species. The intactness of amyloid structures is further confirmed by TEM analysis. Melanin-like species without IHY fibers show amorphous and spherical structures regardless of the presence of Cu^{II}, consistent with other polydopamine-related studies. On the other hand, the addition of IHY or Cu^{II}-IHY results in the formation of thick fibrillar structures encapsulated by dark melanin-like species (Figure 4b). Such fibrillar composites are much thicker (100−200 nm) than the original IHY fibers, proving that multiple fibers are bundled together. The presence of IHY fibers thus likely results in the formation of molecularly more compact and rigid structures taking advantage of the superior mechanical properties of amyloid fibers. It is also relevant to the result that IHY-containing melanin-like species are better dispersible in aqueous solutions, while the absence of fibers results in those strongly adhered to external liquid−solid interfaces.

To examine unpaired electrons and the coordination environment of Cu^{II} and Cu^{II}-IHY in melanin-like species, we conducted electron paramagnetic resonance (EPR) spectroscopy. In general, the EPR measurements were employed to determine the nature, spin-state, oxidation state, and structure (geometry) of paramagnetic species including radical species. The EPR signals of paramagnetic species appear with a certain g factor, which could be coupled with a nuclear spin of paramagnetic species resulting in the splitting of each EPR signal into multiple signals in isotropic electron Zeeman and spin-nuclear interaction (e.g., hyperfine coupling interaction). A careful evaluation of the resulting g values and hyperfine coupling constants (A) is required to determine the electronic and structural nature of paramagnetic species.

The EPR spectra of melanin-like species synthesized both with Cu^{II} and Cu^{II}-IHY exhibit axial signals with $g_{//}$ (e.g., ~2.30 for Cu^{II} and 2.22 for Cu^{II}-IHY) > $g_{\perp}$ (e.g., ~2.09 for Cu^{II} and 2.07 for Cu^{II}-IHY) > 2.00, indicating that the half-occupied ground-state orbital is $3d_{x^2-y^2}$ (Figure 5). The same ground state is found in the tetrahedrally elongated Cu^{II} complexes.[37−40] Basically, resolving a four-line parallel hyperfine structure, which is assignable to the coupling of the electron spin with the copper nuclear spin (I = 3/2), can provide information on the coordination environment of polydopamine with Cu^{II} or Cu^{II}-IHY, respectively. Previously, the EPR spectra of the copper complexes in a distorted

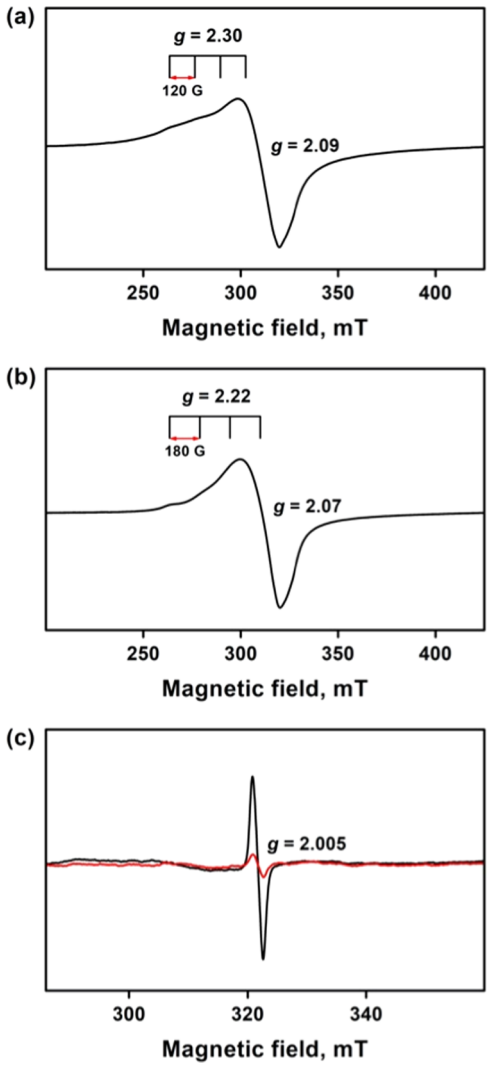

Figure 5. EPR spectra of solid melanin-like species with (a) Cu^{II} and (b) Cu^{II}-IHY. (c) Overlaid EPR spectra of melanin-like species made without any catalyst (red line) and with IHY (black line). Both spectra were collected from the same mass of each sample.

tetrahedral geometry revealed small parallel hyperfine coupling constants ($A_{//}$; e.g., ~60 G), while copper complexes in a square planar geometry displayed larger $A_{//}$ (e.g., >170 G) due to the mixing of $4p_z$ into $3d_{x^2-y^2}$ ground-state wave function or the high degree of covalency of the copper−ligand bond.[38] Interestingly, the $A_{//}$ value of melanin-like species synthesized in the presence of Cu^{II} is determined to be 120 G, whereas that with Cu^{II}-IHY is found to be 180 G (Figure 5a,b). The larger $A_{//}$ value (180 G) of polydopamine with Cu^{II}-IHY compared to that of polydopamine with the Cu^{II} ion (120 G) can be attributed to the different coordination environments around copper, making the contribution of the $3d_{x^2-y^2}$ ground state larger in the presence of IHY fibers. Therefore, melanin-like species with Cu^{II}-IHY are consistent with either a 3N1O or 2N2O coordination environment in a typical square planar geometry, while that with Cu^{II} could be in a fairly distorted square planar geometry.

Regardless of Cu^{II}, melanin-like species contain permanent radical components owing to their molecular constituents containing semiquinone moieties (Scheme 1). These components empower melanin to exhibit superior antioxidant and

https://doi.org/10.1021/acs.langmuir.2c00904
Langmuir 2022, 38, 7077−7084

radical-scavenging activities. As expected, melanin-like species made without Cu^{II} (e.g., authentic melanin-like species and that with IHY) also contain unpaired electrons with the *g* value of 2.0051 ± 0.00005, consistent with the previous results on natural melanin derivatives.[41,42] Surprisingly, the number of stable unpaired electrons is greatly enhanced in the presence of IHY fibers. The relative spin quantification of these signals by integrating them allows us to estimate that the spin density for melanin-like species with IHY fibers is over 10-fold greater than that without IHY fibers (Figure 5c). The difference between actual spin contents in both samples would be larger, since the presence of IHY fibers decreases the relative content of melanin-like species in the same mass. In the case of IHY-Cu^{II}, signals of unpaired electrons in melanin-like species are barely analyzable because of the interference of large Cu^{II} signals. This result suggests that IHY fibers not only accelerate the formation of melanin-like species but also remarkably increase the contents of unpaired electrons therein. Previous studies on natural melanin derivatives have suggested that the spin content and properties of melanin derivatives are highly affected by the way their oligomeric components are aligned before their association.[43] Parallelly aligned β-sheet structures in amyloid fibers provide hydrophobic planar spaces that are prone to accommodate and align nonplanar aromatic organic molecules, such as dihydroxyindole (DHI) and its derivatives, in turn regulating their supramolecular orientation during the process of melanogenesis. Given that the spin density is directly related to the radical-scavenging and antioxidant ability of melanin derivatives, it is reasonable to assume that the amyloid structure of Pmel17 is evolved to have a role in controlling the content of unpaired electrons in the biosynthesis of melanin derivatives.

■ CONCLUSIONS

In summary, we show that a short peptide designed to form amyloid fibers with a Cu^{II}-coordinating capability has multifaceted melanosomal functions in an emergent fashion. In a coordinated form, IHY fibers and Cu^{II} exhibit different functions: (i) IHY fibers have a mild catalytic property for the formation of melanin-like species but largely regulate the morphology and water dispersibility of its final form; (ii) Cu^{II} specifically accelerates the association, likely by catalyzing the initial oxidation of dopamine; (iii) remarkably, melanin-like species synthesized in the presence of IHY fibers contain a significantly higher quantity of unpaired electrons than those without. The detailed relationship between the structure of amyloid fibers and their regulation of spin density in melanin-like species merits further investigation. This work well demonstrates that multifaceted emergent functions can be manifested via the assembly of a supramolecular structure. Artificially designed functions taking advantage of supramolecular structures still fall behind their biological counterparts, and thus more efforts to elucidate naturally occurring emergent functions are necessary.

■ EXPERIMENTAL SECTION

Materials. The IHY peptide (AcNH-IHIHIYI-$CONH_2$) was synthesized manually through the solid-phase peptide synthesis. The Rink Amide MBHA resin HL was purchased from Novabiochem. Piperidine (99%), 0.5 M hydroxyethyl piperazine ethane sulfonic acid (HEPES), pH 8 solution, and 3,5-di-*tert*-butylcatechol (99%) were purchased from Alfa Aesar. Fmoc-protected amino acids and *N*,*N*-diisopropylethylamine (DIPEA, 99%) were purchased from TCI (Japan). Acetic anhydride (99.5%), copper(II) sulfate ($CuSO_4$, 99%), and phosphotungstic acid hydrate ($H_3[P(W_3O_{10})_4]\cdot H_2O$) were purchased from Sigma-Aldrich. *N*,*N*-Dimethylformamide (DMF, 99.0%) for peptide synthesis (99.8%) was purchased from Acros Organics. Trifluoroacetic acid (99.0%), methyl alcohol (HPLC grade), acetonitrile (HPLC grade), water (HPLC grade), dichloromethane (99.5%), and ethyl ether (99.5%) were purchased from Samchun (South Korea).

Peptide Synthesis and Purification. Manual Fmoc solid-phase peptide synthesis was used to synthesize peptides. We used the Rink Amide MBHA resin and the reaction proceeded at room temperature. Fmoc-deprotection was done using a DMF solution of piperidine (20%). The coupling reagent was prepared by mixing Fmoc-protected amino acid, HBTU, and DIPEA in DMF. The coupling reaction took 2 h at room temperature. The Fmoc-deprotection and coupling reactions were repeated for the desired times. N-Terminal was acetylated with acetic anhydride and pyridine in DMF. Cleavage and side-chain deprotection were accomplished by treating the cleavage cocktail, which contains trifluoroacetic acid, triisopropylsilane, and DCM (95:2.5:2.5, v/v), for 2 h at room temperature. The resulting solution was filtered, dried under reduced pressure, and precipitated in diethyl ether. Filtration of the precipitate afforded the crude product, which was then purified using reverse-phase high-performance liquid chromatography with a C18 column (Thermoscientific, 250 × 4.6 mm, 5 μm). The mobile phase was composed of DI water (0.1% of trifluoroacetic acid, v/v; solution A) and CH_3CN (0.1% of trifluoroacetic acid, v/v; solution B). The crude residue was purified with a gradient from 30 to 34% of solution B over 11 min. The lyophilization of the collected fraction afforded the desired product as a white solid (185 mg, 50%). High-resolution mass spectrometry: calculated *m*/*z* (ESI^+) for $C_{47}H_{73}N_{12}O_9$ $[M + H]^+$ = 949.5618, found: 949.5603.

Preparation of Amyloid Fiber. The stock solution was prepared by dissolving purified peptide in a 10 mM HCl solution. The stock solution has no precipitate and thioflavin T signal, indicating that it is in the monomeric state (Figure S6). Concentration was calculated by measuring the absorbance at 280 nm. Cu^{II}-IHY was formed by mixing $CuSO_4$ in water (50 mM), peptide stock solution, and 25 mM HEPES buffer (pH 8.2). The final concentration of peptide in the working solution was 500 μM. To make sure amyloid fiber was formed, the working solution was incubated at 37 °C, 200 rpm. For preparing IHY, $CuSO_4$ was not added to the solution. After 1 h of incubation, the solution was centrifuged (15 000 rpm (20 400 g), 15 min) and the supernatant was replaced by distilled water.

Catechol Oxidation Kinetic Assay. An increase in absorbance, due to the oxidation of substrate 3,5-DBcat, was monitored by a plate reader at 37 °C. The absorbance of five different concentrations of the substrate (0.2, 0.4, 0.8, 1, and 2 mM) at 405 nm was monitored. The 3,5-DBcat stock solution (4 mM) in methanol was prepared freshly before the experiment. The Cu^{II}-IHY solution (500 μM, 7.2 μL) and various volumes of the 3,5-DBcat solution were mixed and finally methanol was added to reach a final volume of 180 μL. The initial rate of the reaction was calculated using the extinction coefficient of 3,5-di-*tert*-benzoquinone (1900 M^{-1} cm^{-1}).[44] The Michaelis−Menten analyses were done by fitting the data to the following equations. We note that the total concentration of the enzyme ($[E_t]$) was set to be same as that of IHY monomer, which would not exquisitely reflect the exact concentration of the actual active sites.

$$V = \frac{V_{max} \times [S]}{K_m + [S]} = \frac{[E_t] \times k_{cat} \times [S]}{K_m + [S]}$$

Synthesis of Melanin-Like Species and a Kinetic Assay of the Reaction. The copper solution was prepared by diluting the $CuSO_4$ stock solution (10 mM) with distilled water until it reached the desired concentrations. The aqueous solutions of Cu^{II}-IHY, Cu^{II}, and IHY were mixed with dopamine solution in a cuvette at various molar ratios. Cuvettes were placed in an orbital shaker (250 rpm) at room temperature. Before measuring the absorbance, cuvettes were carefully agitated for the dispersion of the formed melanin-like

https://doi.org/10.1021/acs.langmuir.2c00904
Langmuir 2022, 38, 7077−7084

species. The kinetic analysis was done by fitting the data to a logistic function

$$A_{450}(t) = A_{max}\left(1 - \frac{1}{1 + \frac{t}{t_0}}\right)$$

where A_{max} is a maximum absorption value and t_0 is the point where the sign of curvature is reversed. The initial velocity of the reaction was obtained by measuring the slope of each spectrum between 0 and 1 h.

Circular Dichroism Spectroscopy. A Jasco J-715 CD spectrometer was used to collect the CD spectra. The sample concentration was 0.4 mg mL^{-1} in 5 mM HEPES (pH 7.8). The measurements were done at room temperature using the continuous scan mode (100 nm/min).

FTIR Spectroscopy. Fibers from Cu^{II}-IHY and IHY were centrifuged (15 000 rpm, 15 min) and the supernatant was discarded. After washing with 25 mM HEPES buffer solution (pH 8.2), the sample was lyophilized. Melanin-like species synthesized with various catalysts were also lyophilized after the supernatant was removed by centrifugation (15 000 rpm, 15 min). All samples were made into a pallet with KBr. The FTIR spectra were collected by Spectrum One System (Perkin-Elmer).

TEM Microscopy. For transmission electron microscopy (TEM) analysis, the salts present in the solution were removed. The sample containing the fibril were be diluted with distilled water. Each sample was placed on a Formvar/carbon 200-coated copper grid. The samples were adsorbed onto the grid for 3 min, washed several times with distilled water, and dried. The grids were stained with 1% phosphotungstic acid hydrate for 5 min, removed from the dye and dried in air. The samples were analyzed using JEM-2100F.

EPR Spectroscopy. EPR spectra were recorded at 80 K using a JEOL X-band spectrometer (JES-FA100) equipped with a cryostat. Four solid samples of melanin-like species formed without a catalyst, with IHY or Cu^{II} or Cu^{II}-IHY, were directly transferred into an EPR tube and flash-frozen in liquid nitrogen. The g value was calibrated using the Mn^{2+} marker, and experimental error in the EPR parameters (g values) was ±0.001. The experimental parameters for EPR measurements were as follows: microwave frequency = 9.025 GHz, microwave power = 0.998 mW, modulation amplitude = 10 G, gain = 1×10^4, modulation frequency = 100 kHz, time constant = 30.96 ms, and conversion time = 85.00 ms.

■ ASSOCIATED CONTENT

Supporting Information

The Supporting Information is available free of charge at https://pubs.acs.org/doi/10.1021/acs.langmuir.2c00904.

HPLC spectra, ESI-MS results, FTIR spectra, UV−vis spectra, result obtained with the excess amount (150 μM) of catalysts (PDF)

■ AUTHOR INFORMATION

Corresponding Authors

Sunbum Kwon − *Department of Chemistry, Chung-Ang University, Seoul 06974, South Korea;* orcid.org/0000-0003-0027-6990; Email: skwon@cau.ac.kr

Seungwoo Hong − *Department of Chemistry, Sookmyung Women's University, Seoul 04310, South Korea;* Email: hsw@sookmyung.ac.kr

Kyungtae Kang − *Department of Applied Chemistry, Kyung Hee University, Yongin, Gyeonggi 17104, South Korea;* orcid.org/0000-0003-4236-8922; Email: kkang@khu.ac.kr

Authors

Hyeyeon Park − *Department of Applied Chemistry, Kyung Hee University, Yongin, Gyeonggi 17104, South Korea*

Hyeri Jeon − *Department of Chemistry, Sookmyung Women's University, Seoul 04310, South Korea*

Min Young Lee − *Department of Applied Chemistry, Kyung Hee University, Yongin, Gyeonggi 17104, South Korea*

Hyojae Jeon − *Department of Applied Chemistry, Kyung Hee University, Yongin, Gyeonggi 17104, South Korea*

Complete contact information is available at: https://pubs.acs.org/10.1021/acs.langmuir.2c00904

Author Contributions

‖H.P. and H.J. contributed equally to the study. K.K., S.H., and S.K. designed the work. H.P., M.Y.L., and H.J. conducted peptide synthesis and catalytic characterizations. H.J. conducted the EPR analysis. H.P. and K.K. wrote the manuscript.

Notes

The authors declare no competing financial interest.

■ ACKNOWLEDGMENTS

This work was supported by the National Research Foundation of Korea (NRF) grant funded by the Ministry of Science, ICT & Future Planning (MSIP) (2019R1C1C1009111 and 2020R1C1C1008886) and the GRRC program of Gyeonggi province [GRRC-kyunghee2017(A01)].

■ REFERENCES

(1) Whitesides, G. M.; Grzybowski, B. Self-assembly at all scales. *Science* **2002**, *295*, 2418−2421.

(2) Robson Marsden, H.; Kros, A. Self-assembly of coiled coils in synthetic biology: inspiration and progress. *Angew. Chem., Int. Ed.* **2010**, *49*, 2988−3005.

(3) Hess, H.; Ross, J. L. Non-equilibrium assembly of microtubules: from molecules to autonomous chemical robots. *Chem. Soc. Rev.* **2017**, *46*, 5570−5587.

(4) Cademartiri, L.; Bishop, K. J. M. Programmable self-assembly. *Nat. Mater.* **2015**, *14*, 2−9.

(5) Zhang, S. G. Fabrication of novel biomaterials through molecular self-assembly. *Nat. Biotechnol.* **2003**, *21*, 1171−1178.

(6) Das, K.; Gabrielli, L.; Prins, L. J. Chemically fueled self-assembly in biology and chemistry. *Angew. Chem., Int. Ed.* **2021**, *60*, 20120−20143.

(7) Dasgupta, A.; Das, D. Designer peptide amphiphiles: self-assembly to applications. *Langmuir* **2019**, *35*, 10704−10724.

(8) Childers, W. S.; Anthony, N. R.; Mehta, A. K.; Berland, K. M.; Lynn, D. G. Phase networks of cross-β peptide assemblies. *Langmuir* **2012**, *28*, 6386−6395.

(9) Chiti, F.; Dobson, C. M. Protein misfolding, functional amyloid, and human disease. *Annu. Rev. Biochem.* **2006**, *75*, 333−366.

(10) Fowler, D. M.; Koulov, A. V.; Balch, W. E.; Kelly, J. W. Functional amyloid-from bacteria to humans. *Trends Biochem. Sci.* **2007**, *32*, 217−224.

(11) Barnhart, M. M.; Chapman, M. R. Curli biogenesis and function. *Annu. Rev. Microbiol.* **2006**, *60*, 131−147.

(12) Hervas, R.; Rau, M. J.; Park, Y.; Zhang, W. J.; Murzin, A. G.; Fitzpatrick, J. A. J.; Scheres, S. H. W.; Si, K. Cryo-EM structure of a neuronal functional amyloid implicated in memory persistence in Drosophila. *Science* **2020**, *367*, 1230−1234.

(13) Salinas, N.; Tayeb-Fligelman, E.; Sammito, M. D.; Bloch, D.; Jelinek, R.; Noy, D.; Uson, I.; Landau, M. The amphibian antimicrobial peptide uperin 3.5 is a cross-alpha/cross-beta chameleon functional amyloid. *Proc. Natl. Acad. Sci. U.S.A.* **2021**, *118*, No. e2014442118.

(14) Maji, S. K.; Perrin, M. H.; Sawaya, M. R.; Jessberger, S.; Vadodaria, K.; Rissman, R. A.; Singru, P. S.; Nilsson, K. P. R.; Simon, R.; Schubert, D.; Eisenberg, D.; Rivier, J.; Sawchenko, P.; Vale, W.; Riek, R. Functional amyloids as natural storage of peptide hormones in pituitary secretory granules. *Science* **2009**, *325*, 328−332.
(15) Rezaei-Ghaleh, N.; Zweckstetter, M.; Morshedi, D.; Ebrahim-Habibi, A.; Nemat-Gorgani, M. Amyloidogenic potential of α-chymotrypsin in different conformational states. *Biopolymers* **2009**, *91*, 28−36.
(16) Calamai, M.; Chiti, F.; Dobson, C. M. Amyloid fibril formation can proceed from different conformations of a partially unfolded protein. *Biophys. J.* **2005**, *89*, 4201−4210.
(17) Knowles, T. P. J.; Mezzenga, R. Amyloid Fibrils as Building Blocks for Natural and Artificial Functional Materials. *Adv. Mater.* **2016**, *28*, 6546−6561.
(18) West, M. W.; Wang, W. X.; Patterson, J.; Mancias, J. D.; Beasley, J. R.; Hecht, M. H. De novo amyloid proteins from designed combinatorial libraries. *Proc. Natl. Acad. Sci. U.S.A.* **1999**, *96*, 11211−11216.
(19) Bolisetty, S.; Arcari, M.; Adamcik, J.; Mezzenga, R. Hybrid amyloid membranes for continuous flow catalysis. *Langmuir* **2015**, *31*, 13867−13873.
(20) Zhang, S.-Q.; Huang, H.; Yang, J.; Kratochvil, H. T.; Lolicato, M.; Liu, Y.; Shu, X.; Liu, L.; DeGrado, W. F. Designed peptides that assemble into cross-α amyloid-like structures. *Nat. Chem. Biol.* **2018**, *14*, 870−875.
(21) Li, D.; Jones, E. M.; Sawaya, M. R.; Furukawa, H.; Luo, F.; Ivanova, M.; Sievers, S. A.; Wang, W. Y.; Yaghi, O. M.; Liu, C.; Eisenberg, D. S. Structure-based design of functional amyloid materials. *J. Am. Chem. Soc.* **2014**, *136*, 18044−18051.
(22) Nguyen, P. Q.; Botyanszki, Z.; Tay, P. K. R.; Joshi, N. S. Programmable biofilm-based materials from engineered curli nanofibres. *Nat. Commun.* **2014**, *5*, No. 4945.
(23) Li, C. X.; Adamcik, J.; Mezzenga, R. Biodegradable nanocomposites of amyloid fibrils and graphene with shape-memory and enzyme-sensing properties. *Nat. Nanotechnol.* **2012**, *7*, 421−427.
(24) Rufo, C. M.; Moroz, Y. S.; Moroz, O. V.; Stohr, J.; Smith, T. A.; Hu, X. Z.; DeGrado, W. F.; Korendovych, I. V. Short peptides self-assemble to produce catalytic amyloids. *Nat. Chem.* **2014**, *6*, 303−309.
(25) Makhlynets, O. V.; Gosavi, P. M.; Korendovych, I. V. Short Self-assembling peptides are able to bind to copper and activate oxygen. *Angew. Chem., Int. Ed.* **2016**, *55*, 9017−9020.
(26) Lengyel, Z.; Rufo, C. M.; Moroz, Y. S.; Makhlynets, O. V.; Korendovych, I. V. Copper-containing catalytic amyloids promote phosphoester hydrolysis and tandem reactions. *ACS Catal.* **2018**, *8*, 59−62.
(27) Zozulia, O.; Korendovych, I. V. Semi-rationally designed short peptides self-assemble and bind hemin to promote cyclopropanation. *Angew. Chem., Int. Ed.* **2020**, *59*, 8108−8112.
(28) Fowler, D. M.; Koulov, A. V.; Alory-Jost, C.; Marks, M. S.; Balch, W. E.; Kelly, J. W. Functional amyloid formation within mammalian tissue. *PLoS Biol.* **2006**, *4*, 100−107.
(29) Watt, B.; van Niel, G.; Fowler, D. M.; Hurbain, I.; Luk, K. C.; Stayrook, S. E.; Lemmon, M. A.; Raposo, G.; Shorter, J.; Kelly, J. W.; Marks, M. S. N-terminal domains elicit formation of functional Pmel17 amyloid fibrils. *J. Biol. Chem.* **2009**, *284*, 35543−35555.
(30) Pfefferkorn, C. M.; McGlinchey, R. P.; Lee, J. C. Effects of pH on aggregation kinetics of the repeat domain of a functional amyloid, Pmel17. *Proc. Natl. Acad. Sci. U.S.A.* **2010**, *107*, 21447−21452.
(31) Watt, B.; van Niel, G.; Raposo, G.; Marks, M. S. PMEL: a pigment cell-specific model for functional amyloid formation. *Pigm. Cell Melanoma Res.* **2013**, *26*, 300−315.
(32) Shin, J. H.; Le, N. T. K.; Jang, H.; Lee, T.; Kang, K. Supramolecular regulation of polydopamine formation by amyloid fibers. *Chem. - Eur. J.* **2020**, *26*, 5500−5507.
(33) Fujieda, N.; Umakoshi, K.; Ochi, Y.; Nishikawa, Y.; Yanagisawa, S.; Kubo, M.; Kurisu, G.; Itoh, S. Copper-oxygen dynamics in the tyrosinase mechanism. *Angew. Chem., Int. Ed.* **2020**, *59*, 13385−13390.
(34) Dreyer, D. R.; Miller, D. J.; Freeman, B. D.; Paul, D. R.; Bielawski, C. W. Elucidating the structure of poly(dopamine). *Langmuir* **2012**, *28*, 6428−6435.
(35) Luo, F. B.; Wu, K.; Shi, J.; Du, X. X.; Li, X. Y.; Yang, L.; Lu, M. G. Green reduction of graphene oxide by polydopamine to a construct flexible film: superior flame retardancy and high thermal conductivity. *J. Mater. Chem. A* **2017**, *5*, 18542−18550.
(36) Coskun, H.; Aljabour, A.; Uiberlacker, L.; Strobel, M.; Hild, S.; Cobet, C.; Farka, D.; Stadler, P.; Sariciftci, N. S. Chemical vapor deposition-based synthesis of conductive polydopamine thin-films. *Thin Solid Films* **2018**, *645*, 320−325.
(37) Iwaizumi, M.; Kudo, T.; Kita, S. Correlation between the hyperfine coupling constants of donor nitrogens and the structures of the first coordination sphere in copper complexes as studied by nitrogen-14 ENDOR spectroscopy. *Inorg. Chem.* **1986**, *25*, 1546−1550.
(38) Shadle, S. E.; Pennerhahn, J. E.; Schugar, H. J.; Hedman, B.; Hodgson, K. O.; Solomon, E. I. X-Ray Absorption spectroscopic studies of the blue copper site-metal and ligand K-edge studies to probe the origin of the EPR hyperfine splitting in plastocyanin. *J. Am. Chem. Soc.* **1993**, *115*, 767−776.
(39) Tano, T.; Ertem, M. Z.; Yamaguchi, S.; Kunishita, A.; Sugimoto, H.; Fujieda, N.; Ogura, T.; Cramer, C. J.; Itoh, S. Reactivity of copper(II)-alkylperoxo complexes. *Dalton Trans.* **2011**, *40*, 10326−10336.
(40) Oh, H.; Ching, W. M.; Kim, J.; Lee, W. Z.; Hong, S. Hydrogen Bond-Enabled Heterolytic and Homolytic Peroxide activation within nonheme copper(II)-alkylperoxo complexes. *Inorg. Chem.* **2019**, *58*, 12964−12974.
(41) Mostert, A. B.; Powell, B. J.; Pratt, F. L.; Hanson, G. R.; Sarna, T.; Gentle, I. R.; Meredith, P. Role of semiconductivity and ion transport in the electrical conduction of melanin. *Proc. Natl. Acad. Sci. U.S.A.* **2012**, *109*, 8943−8947.
(42) Ju, K. Y.; Lee, J. W.; Im, G. H.; Lee, S.; Pyo, J.; Park, S. B.; Lee, J. H.; Lee, J. K. Bio-Inspired, Melanin-Like Nanoparticles as a Highly efficient contrast agent for T-1-weighted magnetic resonance imaging. *Biomacromolecules* **2013**, *14*, 3491−3497.
(43) Panzella, L.; Gentile, G.; D'Errico, G.; Della Vecchia, N. F.; Errico, M. E.; Napolitano, A.; Carfagna, C.; d'Ischia, M. Atypical structural and pi-electron features of a melanin polymer that lead to superior free-radical-scavenging properties. *Angew. Chem., Int. Ed.* **2013**, *52*, 12684−12687.
(44) Neves, A.; Rossi, L. M.; Bortoluzzi, A. J.; Mangrich, A. S.; Haase, W.; Werner, R. Synthesis, structure, physicochemical properties and catecholase-like activity of a new dicopper(II) complex. *J. Braz. Chem. Soc.* **2001**, *12*, 747−754.

https://doi.org/10.1021/acs.langmuir.2c00904
Langmuir 2022, 38, 7077−7084